Novel Ti_3Sn based high damping material with high strength

J. S. Zhang[1], L. S. Cui*[1], C. Yu[1], Y. Shao[1], Z. Q. Wang[1], Y. D. Ru[1], G. Zhang[1], D. Q. Jiang[1], Y. Huan[2] and Y. Ren[3]

In this paper, ductile β-Ti was selected to toughen brittle high damping intermetallic compound Ti_3Sn. An *in situ* Ti_3Sn/β-Ti composite with a composition of $Ti_{77}Mo_3Sn_{20}$ was prepared by arc melting. The composite simultaneously exhibited high yield strength (500 MPa), large plasticity (35%) and high damping capacity (tan $\delta > 0{\cdot}06$). *In situ* synchrotron high energy X-ray diffraction compression testing revealed that the β-Ti mainly accounts for the plasticity, while Ti_3Sn provided the strength of the composite.

Keywords: Damping, Ti_3Sn, Synchrotron

Introduction

Vibrations exist not only in large structures such as aircraft but also in small structures such as electronics, which are harmful for position control, structural stability and noise reduction.[1–3] High damping materials can convert the mechanical energy of vibration into heat, thus eliminating noise and vibration effectively, and are finding increasing applications in mechanical structures.[3–5] Apart from thermoelastic damping, the majority of damping mechanisms in metallic materials relate to the stressn induced movement of crystalline defects.[6] Planar defects (such as twin boundaries) give rise to higher damping levels than point defects and dislocations.[6] Mn–Cu based high damping alloys[7,8] and NiTi[9,10] shape memory alloys are two of the most important and commonly used metallic damping materials whose mechanisms are mainly based on the movement of twin boundaries under external stress. However, existing damping materials cannot meet the needs of the technique progress. It would therefore be of great interest to identify new materials with higher damping capacity.

Vdovychenko *et al.*[11] reported that the intermetallic compound Ti_3Sn shows unusually strong mechanical damping from 1 to 200 Hz, and also from 20 to 100 kHz. At low frequencies, the damping remains high in the temperature range 125–473 K.[11] Although the damping mechanisms of Ti_3Sn intermetallic compounds are still unknown, it has important application potential due to higher damping than the commercial Mn–Cu based damping alloys.[7–8] Nevertheless, owing to a lack of adequate slip systems, Ti_3Sn is very brittle, severely restricting its application as a high damping material.[12] Thus, enhancing the plasticity of Ti_3Sn has become a key topic. In this paper, based on the Ti–Sn binary phase diagram, Mo was selected to stabilise the β-Ti phase, which can improve the plasticity of Ti_3Sn. The obtained Ti_3Sn/β-Ti composite presents not only high strength and large plasticity, but also excellent damping capacity.

Experimental methods

An alloy ingot with nominal composite of $Ti_{77}Mo_3Sn_{20}$ was produced from high purity components (Ti 99·99 wt-%, Mo 99·99 wt-% and Sn 99·99 wt-%) by arc melting using a furnace with a tungsten electrode on a water cooled copper hearth in an argon atmosphere. To achieve chemical homogeneity, the alloy was re-melted five times. After melting, the ingot was furnace cooled. The microstructure of the alloy was analysed by a FEI-200F scanning electron microscope (SEM). Cylindrical compression samples of 5 mm in diameter and 10 mm in length were prepared and tested using a servo-hydraulic materials testing system (MTS 810) with a strain rate of 1×10^{-3} s^{-1} at room temperature. The damping capacity of the alloy was measured using a dynamic mechanical analyser (DMA Q800, TA) in three-point bending mode. The dimension of damping specimens was $1 \times 2 \times 40$ mm (thickness × width × length), and the damping tests were conducted at a frequency of 1 Hz at the temperature range −120 to 150°C, with a constant heating rate of 5°C min^{-1}. *In situ* synchrotron high energy X-ray diffraction (HEXRD) measurement during compression testing was performed at the 11-ID-C beam line of the Advanced Photon Source at the Argonne National Laboratory, USA. Two-dimensional (2D) diffraction patterns in transmission configuration at different applied stresses were collected from the high energy X-rays with an energy of 115 keV, beam size of $0{\cdot}6 \times 0{\cdot}6$ mm and wavelength of 0·10798 Å.

Results and discussion

Figure 1*a* reveals the HEXRD pattern of the $Ti_{77}Mo_3Sn_{20}$ alloy. The main diffraction peaks can be identified as a mixture of a β-Ti solid solution and a Ti_3Sn intermetallic compound. Figure 1*b* shows the SEM backscatter electron image of the alloy. The grey

[1]Department of Materials Science and Engineering, China University of Petroleum, Beijing 102200, China
[2]State Key Laboratory of Nonlinear Mechanics (LNM), Institute of Mechanics, Chinese Academy of Sciences, Beijing 100190, China
[3]X-ray Science Division, Argonne National Laboratory, Argonne, IL 60439, USA

*Corresponding author, email lishancui63@126.com

Received 22 September 2013; accepted 30 January 2014
DOI 10.1179/1432891714Z.000000000750

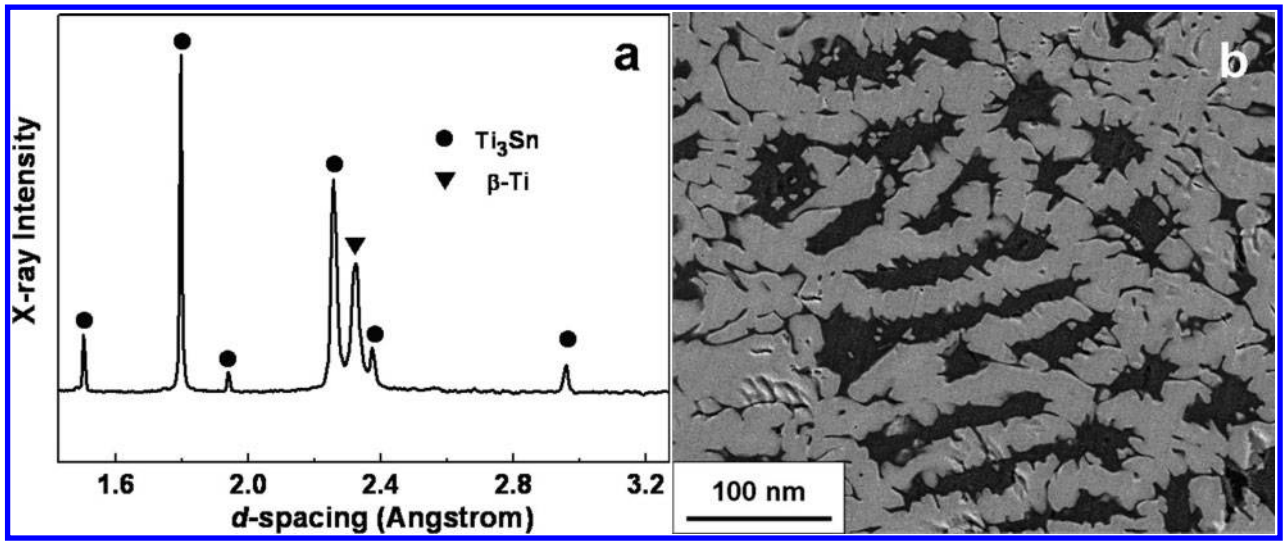

1 ***a*** **HEXRD pattern and** ***b*** **SEM image of as cast $Ti_{77}Mo_3Sn_{20}$ alloy**

dendrite phase represents Ti_3Sn, while the dark phase is β-Ti. Quantitative analysis of the SEM image of the microstructure morphology of the sample studied displays that the volume fraction of the Ti_3Sn phase is about 82%.

The temperature-dependent variation of damping capacity (indexed by tan δ) and storage modulus of the $Ti_{77}Mo_3Sn_{20}$ alloy measured by DMA is shown in Fig. 2. Two damping peaks can be seen in the DMA curve. The first peak extends from 20 to 60°C, while the second peak is in the range –70 to –20°C. The storage modulus soften occurs in the first damping peak, which is different from the second damping peak. The modulus soften may be related to the phase transformation suggested by Vdovychenko *et al*. However, the specific mechanisms of the second damping peak remain unknown. Interestingly, the $Ti_{77}Mo_3Sn_{20}$ alloy exhibits a very high damping capacity at low temperature, with the maximum tan δ reaching 0·08. It is worth noting that the damping is accompanied by an anomaly of the storage modulus as a function of temperature. Contrary to general belief, the damping capacity is inversely related to modulus. However, the damping of the $Ti_{77}Mo_3Sn_{20}$ alloy increases with an increase in the modulus at low temperature. Although this unique phenomenon is not the main focus of this paper, further study of it would be useful. The damping capacity of the $Ti_{77}Mo_3Sn_{20}$ alloy mainly results from the Ti_3Sn intermetallic compound.

The engineering stress–strain curves of the as cast $Ti_{77}Mo_3Sn_{20}$ alloy obtained from uniaxial compression tests under quasi-static loading is shown in Fig. 3. The alloy exhibits yield strength of about 500 MPa and 2% yield strain. The ultimate stress can reach 1100 MPa, while the fracture strain is 35%. Obvious work-hardening is evident. We should note that extensive plasticity was present in an alloy that consists of 82 vol.-% of the normally highly brittle intermetallic compound Ti_3Sn.

In order to uncover the strength and plasticity of the $Ti_{77}Mo_3Sn_{20}$ alloy during compressive testing, *in situ* HEXRD was used to investigate the deformation behaviour. The changes in the 2D diffraction patterns unrolled along the corresponding azimuthally angle from 0 to 360° at different compressive strains provide quantitative information about the structural evolution (see Fig. 4). The obtained alloy sample consists of tens of micrometresized coarse grains oriented in arbitrary directions, indicated by discrete spots on the discontinuous Debye–Scherrer rings in Fig. 4*a*. At 0% applied strain, the corresponding azimuthally unrolled diffraction image (Fig. 4*a*) has straight lines, implying an undeformed (stress-free) state. When the compressive

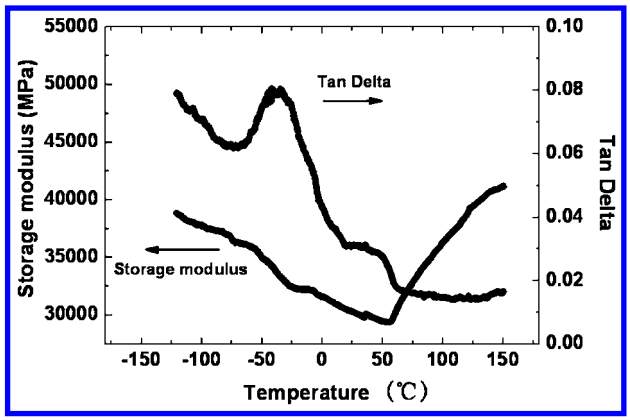

2 Curve (DMA) of as cast $Ti_{77}Mo_3Sn_{20}$ alloy

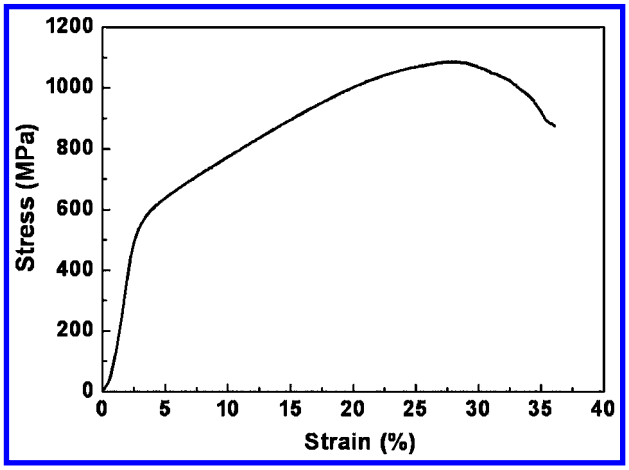

3 Room temperature compressive engineering stress–strain curves of as cast $Ti_{77}Mo_3Sn_{20}$ alloy

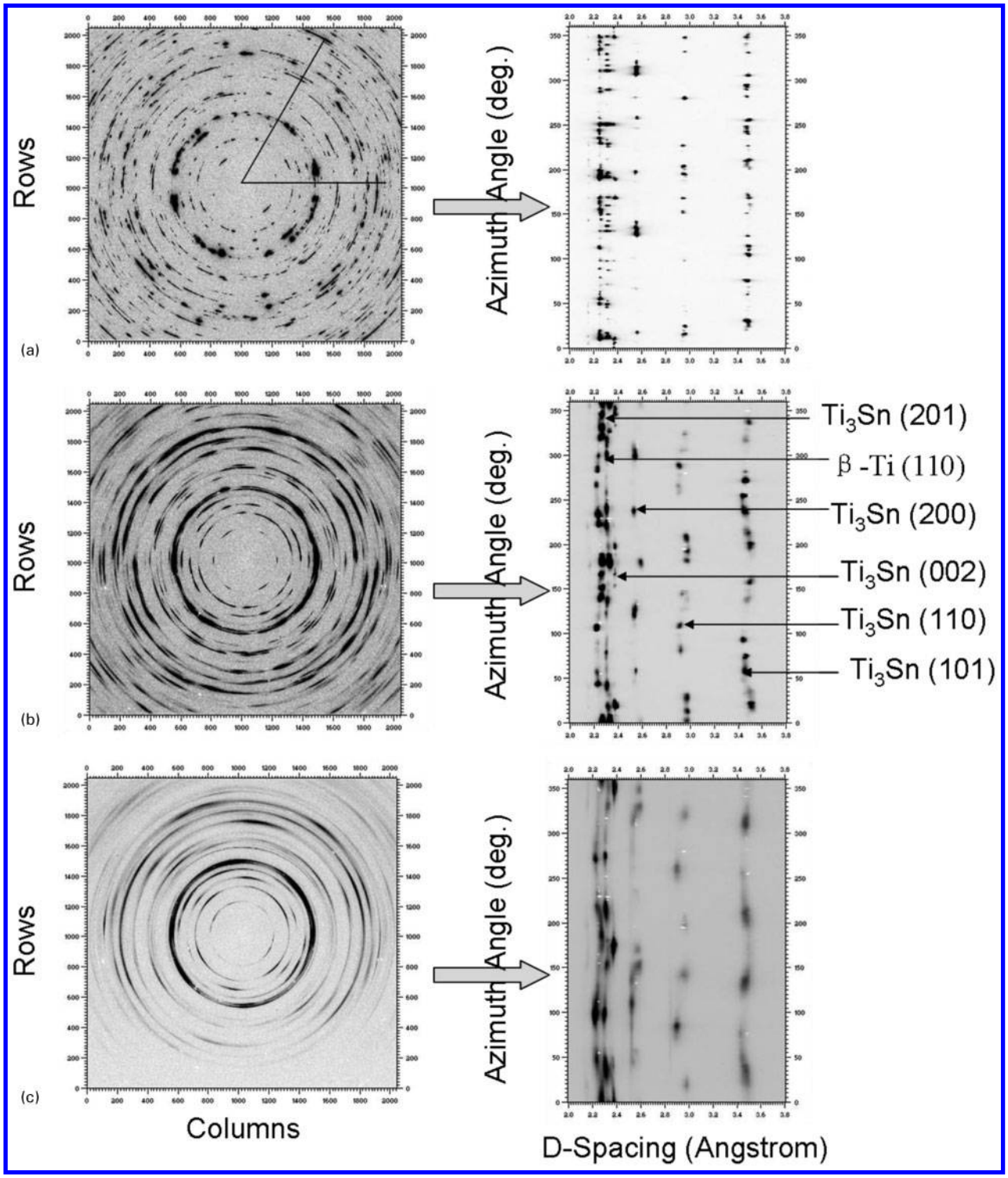

a 0%; *b* 17·4%; *c* 33%

4 *In situ* HEXRD 2D diffraction patterns and corresponding azimuthally (0–360°) unrolled diffraction images of $Ti_{77}Mo_3Sn_{20}$ alloy under different compressive strains

strain is increased, the corresponding azimuthally unrolled diffraction image in Fig. 4*b* reveals variations in the diffraction peak position with respect to the azimuthal angle, indicating that the sample is subjected to compressive stress. The bend of the unrolled diffraction lines results from the elastic deformation of the lattice. After tension, the diffraction patterns change into highly textured, smooth curves, as seen in Fig. 4*c*. It can be seen that the β-Ti (110) diffraction line becomes wide when the strain is increased, which results from the formation of substructure and subgrains from an increasing dislocation density. However, for Ti_3Sn, some of the diffraction spot disappears during the deformation process, indicating the grain rotation is driven by the integrated force from neighbouring grains. The brittle Ti_3Sn interacts with ductile β-Ti, eventually leading to the large plasticity of the $Ti_{77}Mo_3Sn_{20}$ alloy.

The one-dimensional HEXRD diffraction patterns for the stress-free (before loading) and ultimate macrostress states with the diffraction lattice plane perpendicular to

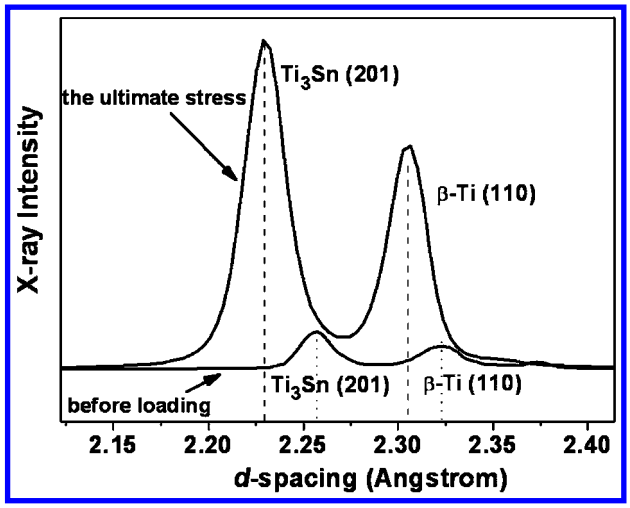

5 One-dimensional HEXRD diffraction profile of alloy in stress-free (before loading) and ultimate stress state along loading direction

the loading direction during compression testing are displayed in Fig. 5. Ti_3Sn (201) and β-Ti (110) peaks shift to lower d-spacing after deformation. The variation of diffraction intensity is caused by the texture. The lattice strain for the reflection peak was calculated using $|d_{hkl}–d_{hkl}^0|/d_{hkl}^0$, where d_{hkl}^0 is the 'stress-free' lattice parameter (i.e. the peak position at zero applied stress). We obtained that the lattice strain of the Ti_3Sn phase and β-Ti (110) phase in the alloy is up to 1·2 and 0·77%, respectively. Because the elastic modulus of Ti_3Sn is higher than for β-Ti, the strength of Ti_3Sn in the alloy exceeds that of β-Ti. Thus, the strength of the alloy stems from intermetallic compound Ti_3Sn, while the β-Ti provides the plasticity.

Conclusions

In conclusion, the incorporation of soft β-Ti that can easily be deformed in combination with brittle Ti_3Sn enhances the plasticity of the $Ti_{77}Mo_3Sn_{20}$ alloy. The Ti_3Sn in the alloy exhibits a higher elastic strain than the β-Ti matrix, and contributes to the strength. The β-Ti phase coordinates the deformation the Ti_3Sn, and results in the grain rotation of Ti_3Sn, resulting in the plasticity of the alloy.

Acknowledgements

This work was financially supported by the National Natural Science Foundation of China (NSFC) (Grant No. 51071175) and the Key (key grant) Project of Chinese Ministry of Education (Grant No. 313055). The use of the Advanced Photon Source was supported by the US Department of Energy, Office of Science and Office of Basic Energy Science under contract no. DE-AC02-06CH11357.

References

1. R. Schaller: *J. Alloys Compd*, 2003, **355**, 131–135.
2. H. Lu, X. Wang, T. Zhang, Z. Cheng and Q. Fang: *Materials*, 2009, **2**, 958–977.
3. D. D. L. Chung: *J. Mater. Sci.*, 2001, **36**, 5733–5737.
4. K. K. Jee, W. Y. Jang, S. H. Baik and M. C. Shin: *Mater. Sci. Eng. A*, 1999, **A273–A275**, 538–542.
5. I. Yoshida, D. Monma and T. Ono: *J. Alloys Compd*, 2008, **448**, 349–354.
6. F. Yin, S. Iwasaki, D. Ping and K. Nagai: *Adv. Mater.*, 2006, **18**, 1541–1544.
7. Q. Tian, F. Yin, T. Sakaguchi and K. Nagai: *Mater. Sci. Eng., A*, 2006, **442**, 433–438.
8. Q. Tian, F. Yin, T. Sakaguchi and K. Nagai: *Acta Mater.*, 2006, **54**, 1805–1813.
9. Y. Chen, H. C. Jiang, S. W. Liu, L. J. Rong and X. Q. Zhao: *J. Alloys Compd*, 2009, **482**, 151–154.
10. D. S. Li, X. P. Zhang, Z. P. Xiong and Y. W. Mai: *J. Alloys Compd*, 2010, **490**, L15–L19.
11. O. V. Vdovychenko, M. V. Bulanova, Y. V. Fartushna and A. A. Shcheretsky: *Scr. Mater.*, 2010, **62**, 758–761.
12. T. Hashimoto, M. Nakamura and S. Takeuchi: *Mater. Trans. JIM*, 1990, **31**, 195–199.